Journal of Organometallic Chemistry 949 (2021) 121957

Contents lists available at ScienceDirect

Journal of Organometallic Chemistry

journal homepage: www.elsevier.com/locate/jorganchem

How acid can become a dihydrogen complex in water? A DFT study

Manuel A. Ortuño [a,*], Agustí Lledós [b,*]

[a] Centro Singular de Investigación en Química Biolóxica e Materiais Moleculares (CIQUS), Universidade de Santiago de Compostela, 15782 Santiago de Compostela, Spain

[b] Departament de Química, Universitat Autònoma de Barcelona, 08193 Cerdanyola del Vallès, Barcelona, Catalonia, Spain

ARTICLE INFO

Article history:
Received 30 April 2021
Revised 16 June 2021
Accepted 17 June 2021
Available online 21 June 2021

Keywords:
Dihydrogen complexes
pK_a
Water solvent
DFT calculations
Discrete-continuum solvation methods

ABSTRACT

To accurate know the acidity of a dihydrogen molecule coordinated to a transition metal ion in water medium is an issue of interest in many areas, from electrochemistry to enzymes and catalysis. However, experimental determination of this magnitude is challenging, and very few values have been reported. In this article we describe a computational protocol, based on DFT calculations and employing a discrete-continuum solvent representation, to estimate pK_a^{water} of transition metal dihydrogen complexes. In this approach the number of solvent molecules explicitly included in the calculations is determined by the convergence with the solvation Gibbs energy of the proton in the solvent. The approach has been initially validated with experimental data in tetrahydrofuran (THF) solvent. Using $(THF)_3$ clusters a mean absolute deviation from experiments of only 1.4 pK_a unit is achieved. In water the convergence is reached with $(H_2O)_{10}$ clusters. Using them in a discrete-continuum model, the pK_a^{water} of twelve dihydrogen complexes experimentally characterized in water have been computed. pK_a^{water} values span a wide range, from 23 to -4, illustrating how coordination to a transition metal modifies the dihydrogen acidity. Decomposition of the ΔG of the acid-base equilibrium in two contributions, one intrinsic to the complex and another one accounting for solvent effects enables a deeper analysis of the dihydrogen acidities.

1. Introduction

Given the imminent consumption of fossil fuels, alternative energy sources such as *the hydrogen economy* should receive the baton. Dihydrogen molecules are not only the feedstock in several hydrogenation processes, but also arise as a potential fuel [1]. Back in the 80s, Kubas et al. reported that transition metals can indeed form σ-complexes binding dihydrogen molecules in a η^2 fashion [2,3]. Since then, a wide variety of dihydrogen complexes have been characterized [4]. In this matter, the production and storage of molecular H_2 are essential concerns that must be addressed, in which transition metals (M) can play a major role [5-9].

The M–H_2 bonding in σ-complexes is usually described using the Dewar-Chatt-Duncanson model, i.e., involving a three-center two-electron interaction stabilized by back donation from a *d* orbital of M to a σ^* orbital of H_2 [10]. The extent of back donation strongly affects the H–H bond distance (0.74 Å in free H_2) giving rise to different stages of dihydrogen species, namely *true* (0.8–1.0 Å), *elongated* (1.0–1.3 Å), and *compressed dihydride* (>1.3 Å) [11,12]. Consequently, the M–H_2 bonding situation can lead to a H–H bond splitting via either homolytic or heterolytic cleavages (Scheme 1). In the homolytic process, the H_2 ligand is oxidatively added to the metal yielding the corresponding dihydride species. Otherwise, in the heterolytic pathway one hydrogen from the H_2 ligand is abstracted as a proton forming a hydride complex [13]. The participation of dihydrogen hydrogen bonded intermediates in this mechanism has been proposed [14-16]. Depending on the location of the base, such a proton transfer can occur intra- or intermolecularly [5-9]. In addition, the heterolytic mechanism is involved in relevant *bio-inspired* processes such as those concerning hydrogenases [17-19].

These heterolytic processes are easily interpreted as acid–base reactions; thus, the evaluation of acid constants K_a (normally expressed as pK_a values) for the coordinated H_2 ligand becomes an invaluable tool. The acidity of free dihydrogen is almost negligible. A first determination of pK_a in tetrahydrofuran (THF) gave a value of 35-37 for dihydrogen [20]. However, more recent estimations are consistent with a pK_a^{THF} of approximately 50 [21]. This value dramatically changes in the presence of transition metals. As pioneering study, Chinn and Heinekey firstly measured the pK_a in acetonitrile of a ruthenium dihydrogen complex, resulting in 17.6 [22]. Since then, a vast collection of experimental values has been

* Corresponding authors.
E-mail addresses: manuelangel.ortuno@usc.es (M.A. Ortuño), agusti@klingon.uab.es (A. Lledós).

https://doi.org/10.1016/j.jorganchem.2021.121957

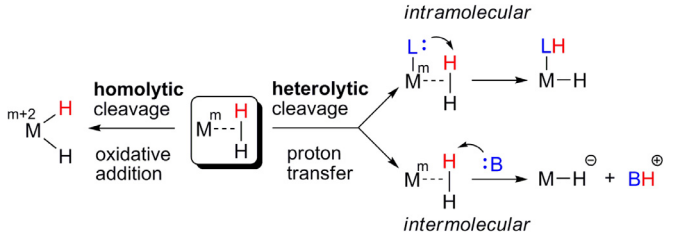

Scheme 1. Transition metal-mediated H–H bond splitting mechanisms

reported in organic solvents [21, 23-33]. Interestingly, some monocationic rhenium [34], dicationic ruthenium [34,35] and osmium [36] species exhibit a remarkably acidic behavior, with pK_a values ranging from −6 to −2. Morris has proposed an empirical, simple equation, based on ligand acidity constants, to estimate the pK_a^{THF} or pK_a^{DCM} values of hydride and dihydrogen species [37]. This simple model has been very successful in accounting and systematizing over 450 reported acid-base reactions involving such species [21]. Density Functional Theory (DFT) calculations have been performed to validate the additive nature of ligand contributions to the pK_a of metal hydride complexes [38-40]. Despite the evident success of the method, it breaks down when specific solvation effects are important as it happen in methanol solvent [21].

Water is a desirable solvent due to its economics and environmental advantages. Despite dihydrogen complexes in organic media have been extensively surveyed [4], these species are difficult to be synthesized and characterized in aqueous environment, hence literature is rather scarce [41]. pK_a measurements in water are neither easy nor straightforward because of solubility issues as well as the leveling effect of the solvent. In those cases in which experimental data are difficult to acquire, theoretical calculations come into play. The computation of acid constants can be performed by computing solvation Gibbs energies [42-45], albeit the proper handling of solvent becomes mandatory to obtain fairly reliable results. Very recently, a data set containing the pK_a of *ca.* 200 transition metal hydrides, computed with low level, semiempirical DFT methods, was used to construct an automated machine learning approach for the rapid estimation of pKa of transition metal hydride complexes [46]. In transition metal chemistry, some examples of pK_a calculations including both implicit and explicit descriptions of the solvent have been reported in organic [47,48] and water [49,50] solvents. Recently, the acidity of methane coordinate to transition metal ions has been investigated with computational methods [51].

Because of the above-mentioned reasons, the acidity of water-soluble transition metal dihydrogen complexes appears as quite interesting feature to get insight into. This work focuses on the experimentally reported water-soluble η^2-H_2 species: *trans*-$[Fe(H_2)(H)(dRpe)_2]^+$ **1** [52] and *trans*-$[Fe(H_2)(Cl)(dRpe)_2]^+$ **2** [53] (R = 3-methoxypropyl), $[CpRu(H_2)(PTA)_2]^+$ **3** and $[Cp^*Ru(H_2)(PTA)_2]^+$ **4** (PTA = 1,3,5-triaza-7-phosphaadamantane) [54,55], *trans*-$[Ru(H_2)(H)(dRpe)_2]^+$ **5** (R = *p*-3-methoxypropylphenyl) [56], *trans*-$[Ru(H_2)(H)(dmpe)_2]^+$ **6** [57], *trans*-$[Ru(H_2)(H)(dppe)_2]^+$ **7** [57], *trans*-$[Ru(H_2)(P(OH)_3)(dppe)_2]^{2+}$ **8** [58], $[Ru(H_2)(H_2O)_5]^{2+}$ **9** [59], $[Os(H_2)(NH_3)_5]^{2+}$ **10** [60,61], *trans*-$[Os(H_2)(Cl)(NH_3)_4]^+$ **11** [60,61], and *trans*-$[Os(H_2)(Cl)(en)_2]^+$ **12** (en = ethylenediamine) [62]. The corresponding conjugated species are: *cis*-$[Fe(H)_2(dRpe)_2]$ **1'**, *trans*-$[Fe(H)(Cl)(dRpe)_2]$ **2'**, $[CpRu(H)(PTA)_2]$ **3'**, $[Cp^*Ru(H)(PTA)_2]$ **4'**, *cis*-$[Ru(H)_2(dRpe)_2]$ **5'**, *cis*-$[Ru(H)_2(dmpe)_2]$ **6'**, *cis*-$[Ru(H)_2(dppe)_2]$ **7'**, *trans*-$[Ru(H)(P(OH)_3)(dppe)_2]^+$ **8'**, $[Ru(H)(H_2O)_5]^+$ **9'**, $[Os(H)(NH_3)_5]^+$ **10'**, *trans*-$[Os(H)(Cl)(NH_3)_4]$ **11'**, and *trans*-$[Os(H)(Cl)(en)_2]$ **12'**. It must be pointed out that the conjugated bases of **1** and **5–7** are *cis*-dihydride species rather than *trans*-derivatives [24,32] likely due to the strong *trans* influence exerted by the two hydride ligands.

The estimation of pK_a values in water is performed after testing the computational protocol in THF, with the final aim of providing valuable information to design transition metal complexes capable of tune the coordinating and splitting properties of H–H bonds.

2. Computational details

2.1. Geometries and energies

Geometries have been fully optimized at the DFT level in gas phase using the M06 density functional [63] (with an ultrafine grid) [64] as implemented in Gaussian 09 [65]. This functional correctly accounts for dispersion interactions and is recommended for transition metal chemistry [66,67] and water clusters [68]. Fe, Ru, and Os atoms were described by means of an effective core potential SDD for the inner electrons and its associated double-ζ basis set for the outer ones [69], complemented with a set of f-polarization functions [70]. The 6-31G(d,p) was used on H atoms, 6-31G(d) on C, N, F, P, and Cl atoms, and 6-31G+(d) on O atoms [71-73]. This setup is now called BI. Geometries were optimized without any symmetry restrictions and the nature of the minima has been verified with analytical frequency calculations. All transition metal complexes present closed shell electronic structures (singlet spin state). Gibbs energy calculations have been performed at 298.15 K and 1 atmosphere. Single point calculations were performed on previous gas-phase (g) geometries (computed at M06/BI level) using 6-311++G(d,p) on H, C, N, O, F, P, Cl atoms [74-76], namely, setup BII. $\Delta G_{gp}(BII)$ was obtained by adding the BI-entropic contribution to $\Delta E_{gp}(BII)$:

$$\Delta G_g(BII) = \Delta E_g(BII) + [\Delta G_g(BI) - \Delta E_g(BI)] \quad (1)$$

Tetrahydrofuran (THF, ε = 7.43) and water (ε = 78.36) solvents (sol) have been described as a continuum using the SMD method [77]. Single point calculations in solvent were carried out using the BII setup and $\Delta G_{sol}(BII)$ values were deduced by adding the BI-entropic contribution to $\Delta E_{sol}(BII)$:

$$\Delta G_{sol}(BII) = \Delta E_{sol}(BII) + [\Delta G_g(BI) - \Delta E_g(BI)] \quad (2)$$

2.2. pK_a computation

Acid constants can be estimated by computing the standard Gibbs energy in solution of the corresponding deprotonation process. To deal with solvation of species, the proper description of the solvent becomes crucial. Especially when solute–solvent interactions may be decisive, such as water [78,79], solvent is described in both implicit (continuum) and explicit (discrete molecules) ways. These methods are commonly known as cluster–continuum [80-82] and implicit–explicit [83].

Several procedures to compute acid constants by means of DFT calculations can be found in literature [42-46]. A recent report showcases the improvement provided by discrete-continuum solvation methods in the pK_a calculations. There are cases where the root mean squared error is as large as 7 pK_a units with pure continuum solvation model and becomes around 1 pK_a unit with the hybrid approach [84]. Accordingly, herein, the calculations are performed by means of a hybrid cluster–continuum approach [81] as shown in Scheme 2 in THF and water. Solvent (S) is treated as cluster configurations of n molecules (S_n and H^+S_n). $\Delta G^o_{g,deprot}$ stands for the deprotonation Gibbs energy in gas phase. The term $\Delta G^{o\rightarrow *}$, which is the conversion factor from an ideal gas standard state of

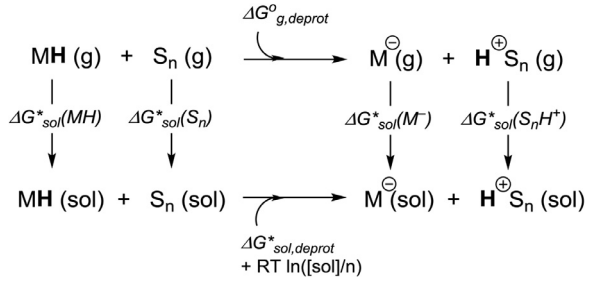

Scheme 2. Cluster-type thermodynamic cycle for deprotonation Gibbs energies in solution

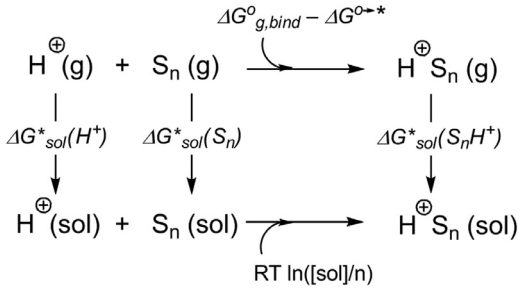

Scheme 3. Cluster-type thermodynamic cycle for the solvation Gibbs energy of proton

1 atm "°" to a standard state of 1 M "*" [85], cancels out since the molecularity of the reaction is zero. $\Delta G^*_{sol}(X)$ terms represent standard solvation Gibbs energies of species X, and RT•ln([sol]/n) is the correction term for the Gibbs energy change of 1 mol of [sol]/n M liquid state to 1 M [86].

According to the thermodynamic cycle illustrated in Scheme 2, the deprotonation Gibbs energy in solution is derived as the following equation:

$$\Delta G^*_{sol,deprot} = \Delta G^\circ_{g,deprot} + \Delta G^*_{sol}(M^-) + \Delta G^*_{sol}(H^+S_n) - \Delta G^*_{sol}(MH) - \Delta G^*_{sol}(S_n) - RT \ln ([sol]/n) \quad (3)$$

and the pK_a can be expressed as:

$$pKasol = \Delta G^*sol,deprot / 2.303\ RT \quad (4)$$

It can be easily deduced from (4) that Gibbs energy errors of 1.4 kcal mol^{-1} entail errors in pK_a of 1 unit at room temperature, being 2 units an acceptable discrepancy [43]. Detailed ΔG values can be found in the Supporting Information.

2.3. Number of solvent molecules

The number of solvent molecules explicitly included in the calculations, n, is that which properly accounts for the solvation Gibbs energy of the proton, $\Delta G^*_{sol}(H^+)$ in Scheme 3 [82].

Accordingly, the $\Delta G^*_{sol}(H^+)$ term is evaluated using:

$$\Delta G^*_{sol}(H^+) = \Delta G^\circ_{g,bind} - \Delta G^{\circ\rightarrow *} - \Delta G^*_{solv}(S_n) + \Delta G^*_{sol}(H^+S_n) - RT \ln ([sol]/n) \quad (5)$$

For the cluster-type thermodynamic cycle (Scheme 3), the actual value of $\Delta G^*_{sol}(H^+)$ is obtained when $n\rightarrow\infty$ [82]. Thus, n is estimated as the number that provides a fairly converged value of $\Delta G^*_{sol}(H^+)$. Experimental values of $\Delta G^*_{sol}(H^+)$ are here mandatory in order to validate the theoretical predictions. In aqueous solution the accepted $\Delta G^*_{water}(H^+)$ is −265.9 kcal mol^{-1} as reported by Tissandier et al. [87-89]. This result has been confirmed by several theoretical studies using cluster–continuum (−266.7 kcal mol^{-1}) [82] and implicit–explicit (−266.1 kcal mol^{-1}) [83] models. Unfortunately, accurate data in non-aqueous solvents is less accessible. For THF solvent, the $\Delta G^*_{THF}(H^+)$ value has been estimated by adding a correction term to $\Delta G^*_{water}(H^+)$, resulting in −256.3 kcal mol^{-1} [47,90]. The number of THF and water molecules considered in this study will be discussed next.

Table 1
Computed and experimental $\Delta G^*_{THF}(H^+)$ values

n	$\Delta G^*_{THF}(H^+)$ / kcal mol^{-1}
1	−242.8
2	−258.8
3	**−260.5**
Exp. [47,90]	−256.3

3. Results and discussion

3.1. Estimating the cluster size

Prior to the calculation of pK_a values, one should evaluate the number of solvent molecules, n, required to properly compute Gibbs energies in Scheme 2. As mentioned before, such number should reproduce the experimentally reported value of $\Delta G^*_{sol}(H^+)$. Several cluster structures S_n and H^+S_n are computed for THF and water solvents.

Small clusters up to 3 molecules are considered for THF solvent. Among the several conformations explored, Fig. 1a displays the most stable $(THF)_{2-3}$ structures. Starting from the dimer $(THF)_2$, the approaching of a third THF molecule generates two main subclasses of conformations for $(THF)_3$, namely, stacked and non-stacked configurations. The non-stacked structure is finally considered, being 0.5 kcal mol^{-1} more stable than the stacked one. On the other hand, Fig. 1b depicts the most relevant $H^+(THF)_{2-3}$ clusters. The proton in species $H^+(THF)_2$ appears strongly solvated by the oxygen atoms, showing O•••H distances of ca. 1.19 Å. The inclusion of a third THF molecule as in $H^+(THF)_3$ forms a weaker interaction with a O•••H distance of 2.651 Å. Consequently, no additional molecules were further considered in order to simplify the conformational space.

The $\Delta G^*_{THF}(H^+)$ values computed using (5) are collected in Table 1 for clusters containing 1–3 THF molecules. As expected, the description using only one molecule is not appropriate, but it significantly improves with the dimer structures. The calculation using clusters with 3 molecules slightly decreases the Gibbs energy by 1.7 kcal mol^{-1} with respect to those with 2, thus convergence is assumed for n = 3. The values of $\Delta G^*_{sol}(H^+(THF)_3)$ and $\Delta G^*_{sol}((THF)_3)$ used in the pK_a computation via (3) are −43.9 and −9.4 kcal mol^{-1}, respectively.

The same protocol is adopted to estimate the number of water molecules. Previous work on water clusters stated that, for even numbers of molecules, $(H_2O)_n$ can be divided into two subclasses, $(H_2O)_{4m}$ and $(H_2O)_{2+4m}$ (m = 1, 2, ...), being the latter more stable [82]. For m > 2, the complex network of hydrogen bonds provides a clustering scenario difficult to deal with [91,92]. Since the full exploration of water configurations is not the goal of this study, only 1–4, 6 and 10 molecules are considered. Fig. 2a shows selected $(H_2O)_n$ clusters for n = 4, 6 and 10. Although the cyclic structure is the most stable conformation for $(H_2O)_4$, it is less clear for $(H_2O)_6$. Binding energies computed using CCSD(T) and MP2 methods favor the prism structure [93]. According to the present level of theory (see Computational Details), energies in gas-phase indeed support

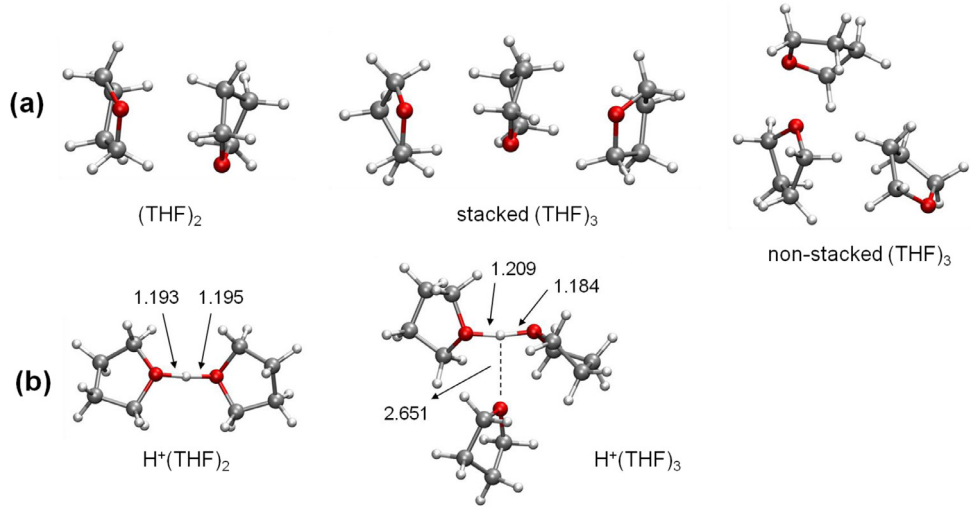

Fig. 1. Optimized structures of (a) $(THF)_n$ and (b) $H^+(THF)_n$, n = 2, 3. Distances in Å.

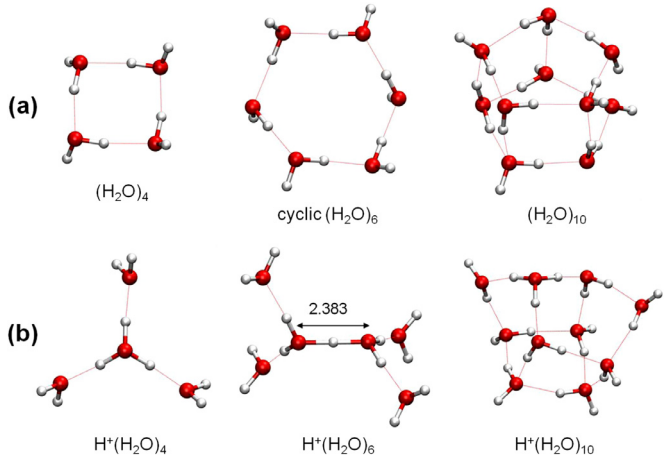

Fig. 2. Optimized structures of (a) $(H_2O)_n$ and (b) $H^+(H_2O)_n$, n = 4, 6 and 10. Distance in Å.

the prism hexamer, but Gibbs energies in solution claim for the cyclic form, being ca. 3–5 kcal mol^{-1} more stable than the prism and cage counterparts. The geometry of $(H_2O)_{10}$ is taken from literature [94]. Likewise, Fig. 2b displays the $H^+(H_2O)_n$ clusters for n = 4, 6 and 10. The structure of $H^+(H_2O)_4$ is interpreted as a H_3O^+ ion solvated by 3 water molecules. Concerning $H^+(H_2O)_6$, among the several configurations explored [95] we found that the disposition experimentally proposed by Reed and co-workers [96-98] is preferred, showing a O•••O distance of 2.383 Å [99]. Analogous to $(H_2O)_{10}$, the geometry of $H^+(H_2O)_{10}$ is collected from literature [83].

The $\Delta G^*_{water}(H^+)$ values computed using (5) are collected in Table 2 for clusters of 1–10 water molecules. Structures with one and two molecules poorly describe the experimental value, although a quite improvement is obtained for n = 3, 4. After expanding the cluster up to 6 and 10 molecules, the result becomes quite better. The difference between $\Delta G^*_{water}(H^+)$ values for 6 and 10 molecules is only 1.2 kcal mol^{-1}, thus convergence is assumed for n = 10. Previous calculations considered 4 [82] and 10 water molecules [83]. The present computed value of −265.7 kcal mol^{-1} is in agreement with the experimental one, −265.9 kcal mol^{-1} [87,88]. The corresponding values of $\Delta G^*_{sol}(H^+(H_2O)_{10})$ and $\Delta G^*_{sol}((H_2O)_{10})$ used in the pK_a computation via (3) are −64.3 and −23.4 kcal mol^{-1}, respectively.

Table 2
Computed and experimental $\Delta G^*_{water}(H^+)$ values

n	$\Delta G^*_{water}(H^+)$ / kcal mol^{-1}
1	−249.8
2	−255.4
3	−262.4
4	−263.5
6	−264.5
10	**−265.7**
Exp. [87,88]	−265.9

3.2. Calibrating the method: computing pK_a in THF

The present study pursues the pK_a computation of dihydrogen species in water, particularly **1**–**12**. Although hybrid cluster–continuum methods perform generally well for such calculations, no dihydrogen complexes have been analyzed so far, thus an initial validation with respect to experimental data is recommended. Unfortunately, no experimental data of **1**–**12** are available in aqueous solution. Instead, the pK_a values have been evaluated in THF solution. Consulting the literature of **1**–**12**, only the pK_a^{THF} of **7** has been measured [31]. The analysis is then extended to include other complexes which pK_a^{THF} values are reported (Fig. 3): *trans*-$[Ru(H_2)(H)(dArpe)_2]^+$ (Ar = *p*-methoxyphenyl) **13**, *trans*-$[Fe(H_2)(H)(dppe)_2]^+$ **14**, *trans*-$[Os(H_2)(H)(dppe)_2]^+$ **15**, $[CpRu(H_2)(dppm)]^+$ **16**, and $[Cp^*Ru(H_2)(dppm)]^+$ **17** [31]. The conjugated bases are: *cis*-$[Ru(H)_2(dArpe)_2]$ **13**, *cis*-$[Fe(H)_2(dppe)_2]$ **14**, *cis*-$[Os(H)_2(dppe)_2]^+$ **15**, [CpRu(H)(dppm)] **16**, and $[Cp^*Ru(H)(dppm)]$ **17**.

The pK_a^{THF} values of **7** and **13**–**17** are computed according to (3) and (4) using clusters with 3 THF molecules as depicted in Scheme 4. The results are collected in Table 3. The calculations are in fair agreement with the experimental ones [21,37], showing absolute differences in the range of 0.0–2.8 units. This DFT-based protocol is recommended when the subtle influence of remote groups, such as the *p*-OMe groups in **13**, needs to be captured. These positive results suggest that the present computational protocol can be successfully applied to dihydrogen species in THF.

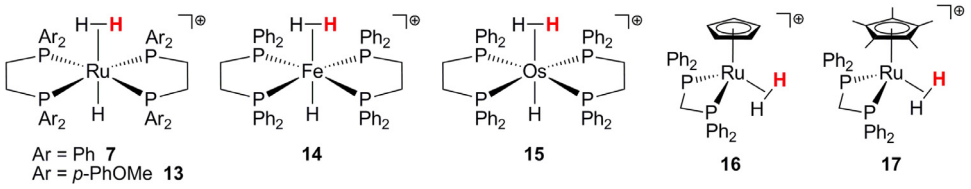

Fig. 3. Dihydrogen complexes studied in THF. 3D pictures of the optimized dihydrogen complexes, as well their related hydrides can be found at the Supporting Information.

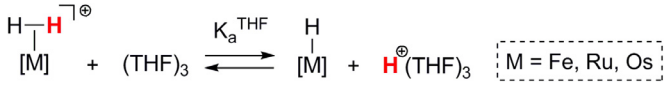

Scheme 4. Model deprotonation reaction of dihydrogen species in THF (n = 3)

Table 3
Calculated and experimental [37] pK_a^{THF}

Species	pK_a^{THF} (calc)	pK_a^{THF} (exp)	$\lvert\Delta pK_a^{THF}\rvert$
7	14.1	14.1	0.0
13	17.9	17.4	0.5
14	14.3	11.5	2.8
15	14.1	12.1	2.0
16	9.6	7.2	2.4
17	9.9	9.2	0.7
MAD[a]			1.4

[a] Mean absolute deviation from experiments.

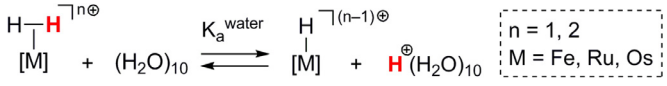

Scheme 5. Model deprotonation reaction of dihydrogen species in water (n = 10)

3.3. Computing pK_a in water

The computational protocol has been previously tested against similar dihydrogen complexes in THF solution. Since the water clusters seem to be adequate (they do reproduce the proton solvation value $\Delta G^*_{water}(H^+)$), we hypothesize that the present discrete-continuum protocol could also be applied to dihydrogen complexes in water. The pK_a^{water} values of **1**–**12** have been estimated according to (3) and (4) using clusters with 10 water molecules as depicted in Scheme 5. The values for each complex are collected in Fig. 4, ranging from 23.0 in **12** to −3.5 in **8**. The corresponding H–H bond distances have also been gathered in Fig. 4. Complexes **1**–**10** display values of 0.8–0.9 Å, whereas **11** and **12** behave as elongated dihydrogen species, showing distances of 1.2–1.3 Å.

To gain further insight into the acidic properties, Equations (3) and (4) can be combined to express pK_a^{water} (4) according to two main terms, $\Delta G^\circ_{g,deprot}$ and $\Delta\Delta G^*_{sol}$:

$$pK_a^{water} = (\Delta G^\circ_{g,deprot} + \Delta\Delta G^*_{sol} + \text{constant}) / 2.303\ RT \quad (6)$$

$\Delta G^\circ_{g,deprot}$ represents the thermodynamics of the deprotonation reaction in gas phase, i.e., the intrinsic acidity of the H_2 ligand in the transition metal complex. On the other hand, $\Delta\Delta G^*_{sol}$ accounts for the solvation Gibbs energy difference between products and reactants. This means that the relative stability of species mainly comes from implicit solvation effects (as the proton in gas phase is already solvated with explicit solvent molecules).

The $\Delta G^\circ_{g,deprot}$ and $\Delta\Delta G^*_{sol}$ contributions for each complex are illustrated in Fig. 5 as blue and red bars, respectively. For monocationic species **1**–**7, 11**, and **12**, the positive values of $\Delta G^o_{g,deprot}$ show the difficulty to deprotonate the dihydrogen complexes to form the hydride derivatives. For the other term, $\Delta\Delta G^*_{sol}$, all contributions are negative and relatively small in the range of 2–14 kcal mol^{-1}.

Due to the systematic effect of $\Delta\Delta G^*_{sol}$, the $\Delta G^o_{g,deprot}$ term mainly governs the acidity. Conversely, dicationic species **8**–**10** behave the other way around, i.e., they exhibit negative values of $\Delta G^o_{g,deprot}$; in other words, the deprotonation of such dicationic complexes is thermodynamically favored. The solvation term $\Delta\Delta G^*_{sol}$ also works in the opposite direction with respect to monocations; positive values indicate that the solvation of dicationic dihydrogen reactants becomes more relevant than that involving monocationic hydride and $H^+(H_2O)_{10}$ products. The scarce number of reported dicationic species hampers a proper analysis of general trends.

The $\Delta\Delta G^*_{sol}$ term seems to be rather similar for the monocationic species under study. As a consequence, a direct correlation between pK_a^{water} and $\Delta G^o_{g,deprot}$ can be found. The corresponding plot of pK_a^{water} against $\Delta G^o_{g,deprot}$ is shown in Fig. 6. The calculated regression line (R^2 = 0.863) affords a slope of 0.59. Assuming $\Delta\Delta G^*_{sol}$ as a constant in (6), the resulting ideal slope shall be 0.73 (298 K), which is close to the present value of 0.59. Overall, for these monocationic species the acidity of the dihydrogen ligand can be roughly estimated in the basis of the gas-phase deprotonation term $\Delta G^o_{g,deprot}$.

3.4. Discussing pK_a in water

This section is devoted to discuss the pK_a^{water} results obtained for the transition metal complexes **1**–**12**. As regards the geometrical parameters, one important feature may be the H–H bond distance of dihydrogen ligands (Fig. 4), although no global correlation toward the acidity is found. That is, the elongated nature of dihydrogen ligands apparently does not influence the acidic behavior in a systematic way. Complexes **1**–**12** will be analyzed regarding the transition metal as follows.

For the Fe-based species *trans*-$[Fe(H_2)(X)(dRpe)_2]^+$, the pK_a^{water} of **1** (X = H) and **2** (X = Cl) are 20.4 and 12.8, respectively. The difference results in 7.6 units and mainly comes from the gas-phase deprotonation term ($\Delta G^o_{g,deprot}$ of 8.4 kcal mol^{-1}). Notably, **1′** adopts a *cis* rearrangement of phosphines whereas **2′** maintains the *trans* stereochemistry. Morris and co-workers have reported similar results for a set of *trans*-$[Os(H_2)(X)(dppe)_2]^+$ complexes in dichloromethane solution. For X = H [24] Cl, and Br ligands [25], the pK_a values are 13.6, 7.4, and 5.4, respectively. The ΔpK_a between the Os-based complexes with H and Cl ligands is 6.2, in line with the 7.6 units previously mentioned for the Fe-derivatives **1** and **2**.

Moving forward to Ru-based species **3**–**7**, some differences are revealed according to the ligands presented. Within the same family, more electron-donating ligands correlate to larger pK_a^{water}. For instance, the pK_a^{water} of Cp-derivative **3** is 1.3 units lower than that of Cp*-derivative **4** [100]. This trend shown by Cp and Cp* ligands has been experimentally detected for **16** and **17** (ΔpK_a^{THF} of 2.0 in Table 3) [21,37] and other related species [23]. A similar but more stressed trend is observed for the pK_a^{water} values of bis(phosphine) complexes *trans*-$[Ru(H_2)(H)(dXpe)]^+$, being **7** (X = Ph, 12.3) quite more acidic than **6** (X = CH_3, 19.3), and **6** more acidic than **5**

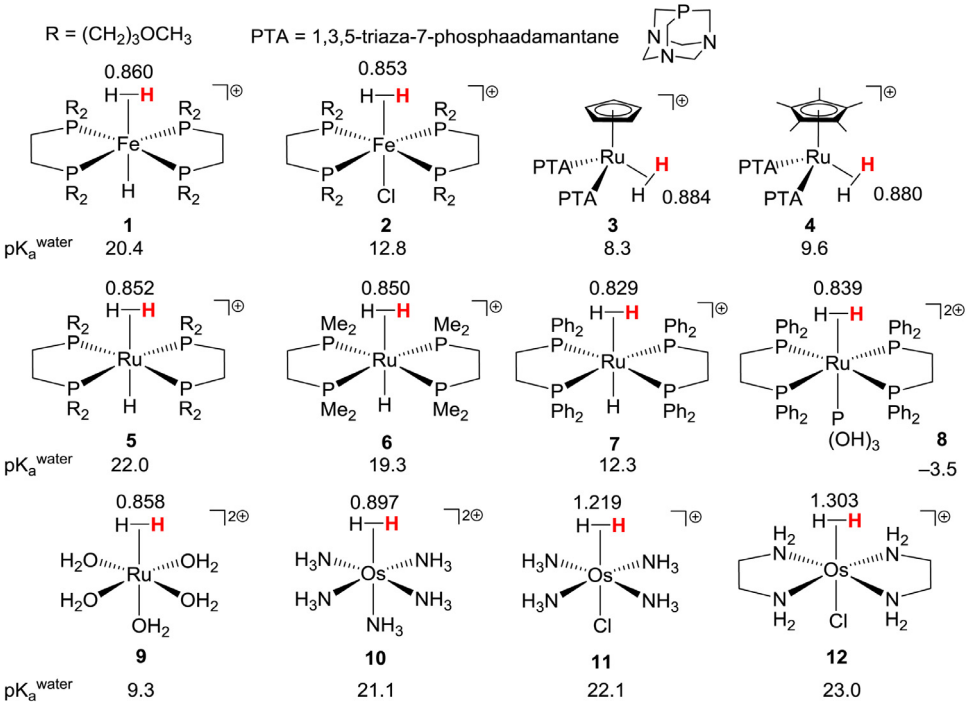

Fig. 4. pK_a^{water} and H–H bond distances (in Å) of dihydrogen species **1**–**12**. 3D pictures of the optimized dihydrogen complexes, as well their deprotonated hydrides (**1'-12'**), are collected in the Supporting Information.

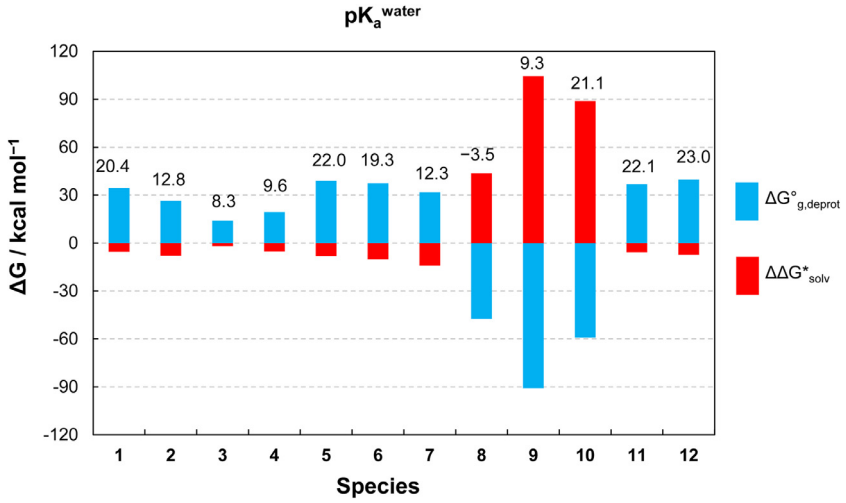

Fig. 5. Bar chart showing ΔG contributions for species **1**–**12**, including pK_a^{water} values.

(X = $(CH_2)_3OCH_3$, 22.0). In these cases the steric and electronic properties are not fully separated. As computational exercise, some complexes of the type [Ru–(dmpe)] are calculated substituting methyl groups by H **18**, CF_3 **19** and F **20** (Scheme 6), where steric contributions are rather similar among them but electronic effects are not. In this scenario, electron-withdrawing groups clearly enhance the acidity of dihydrogen complexes. The pK_a^{water} values range from 19.3 in **6** (X = CH_3) to −4.4 in **20** (X = F). In other words, the more electron-donating the ligands are, the less acidic the complex behave [30]. The chelating size of the bis(phosphine) ligands may also influence [101,102].

An interesting scenario arises for complex **8**, which exhibits superacidic properties according to the calculated pK_a^{water} of −3.5. The dicationic nature is indeed a key factor, but it is worth noting that dicationic complexes do not entail a strong acidic character systematically, see for instance the Os-derivatives **9** (9.3) and **10** (21.1). Other dihydrogen complexes acting as strong acids have been reported, e.g., monocationic $[Cp^*Re(H_2)(CO)(NO)]^+$ (pKa ca. −2) [34] and dicationic *trans*-$[Os(H_2)(CO)(dppp)_2]^{2+}$ (pKa ca. −5.7) [35] and *trans*-$[Os(H_2)(CH_3CN)(dppe)_2]^{2+}$ (pKa ca. −2) [36]. To further investigate the case of **8**, taking into account the influence of the ligand L *trans* to the dihydrogen ligand in the acidity, the pK_a^{water} values of hypothetical species calculated with other ligands L are displayed in Scheme 7. Inspired by the previous reports [35,36] the $P(OH)_3$ ligand in **8** has been substituted by CH_3CN **21** and CO **22**. In line with above-mentioned

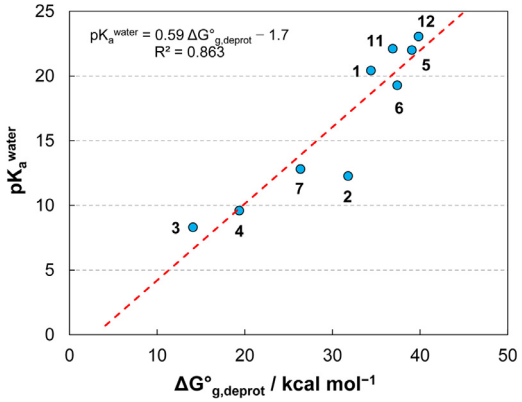

Fig. 6. Plot of pK_a^{water} against $\Delta G°_{g,deprot}$ for monocations **1**–**7**, **11**, and **12**. Regression line in dashed red.

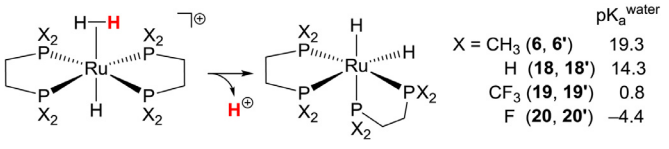

Scheme 6. pK_a^{water} of complexes **18**–**20** derived from **6**. 3D pictures of the optimized dihydrogen complexes, as well their deprotonated hydrides (**'**), are collected in the Supporting Information.

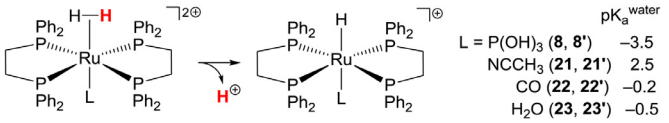

Scheme 7. pK_a^{water} of complexes **21**–**23** derived from **8**. 3D pictures of the optimized dihydrogen complexes, as well their deprotonated hydrides (**'**), are collected in the Supporting Information.

acids, the computed pK_a^{water} values of 2.5 for **21** and −0.2 for **22** clearly account for strong acidic properties. As a matter of fact, a solvent water molecule is also considered as ligand forming **23**. This complex does conserve the acidity, with a pK_a^{water} of −0.5. One can suggest that the acidic behavior of bis(phosphine) complexes mainly comes from their dicationic and phosphine-based nature, since the superacidic behaviour is absent in the dications **9** and **10** containing O- and N-donor ligands, respectively. The type of ligand L also influence but to a less extent.

As concerns the Os-based complexes **10**–**12**, the resulting pK_a^{water} values are rather similar and fewer conclusions can be made. Curiously, the dicationic species **10** exhibit a similar acidic behaviour than monocations **11** and **12**. The latter **12** is slightly less acidic than **11** (0.9 units), presumably due to the better electron-donor properties of primary amine ligands with respect to ammonia.

4. Conclusions

We employed a computational protocol, based on DFT calculations, to estimate pK_a of transition metal dihydrogen complexes in water solvent. We used a discrete-continuum solvation approach, in which the number of solvent molecules explicitly included in the calculations properly accounts for the solvation Gibbs energy of the proton in the solvent at choice. Giving the scarcity of experimentally determined pK_a in water of dihydrogen complexes, the approach has been initially validated with experimental data in THF solvent. Including clusters with three THF molecules, the computed pK_a^{THF} are in fair agreement with the experimental values, displaying a mean absolute deviation from experiments of ca. 1 pK_a unit.

The same protocol has been adopted to estimate the number of water molecules. Convergence on the proton solvation has been achieved for $(H_2O)_{10}$ clusters. Therefore, introducing these clusters in the discrete-continuum model, the pK_a^{water} of twelve experimentally characterized transition metal-dihydrogen complexes have been computed. pK_a^{water} values obtained in this way span a broad range, from 23 to −4, illustrating how coordination to a transition metal is modifying the dihydrogen acidity. Nevertheless, no global correlation between the H–H bond distance of dihydrogen ligand and acidity has been found. To further analyze the acidic properties, we have decomposed ΔG of deprotonation in water of all the complexes in two contributions, one describing the intrinsic acidity of the H_2 ligand ($\Delta G°_{g,deprot}$, thermodynamics of the deprotonation reaction in gas phase) and the other one accounting for implicit solvent effects in the relative stabilities of acid and conjugate basis forms of each complex ($\Delta\Delta G^*_{sol}$). For monocationic species, $\Delta G°_{g,deprot}$ term mainly governs the acidity, being the $\Delta\Delta G^*_{sol}$ term rather similar for all the monocationic species considered. To separate steric and electronic effects, we have varied a X ligand in a series of complexes structurally equivalent, finding a marked influence of the electron-donating properties of X in pK_a^{water}, changing from 19.3 for X = Me to −4.4 for X = F. Within the same family, more-electron donating ligands correlate to higher pK_a^{water}.

Dicationic complexes behave in a different way; for them, the deprotonation is intrinsicality favored (negative $\Delta G°_{g,deprot}$ term). However, the solvation term works in opposite direction, against deprotonation. As a result of the two factors operating in opposite directions, dicationic complexes do not systematically entail a strong acidic character. However, the scarce number of dicationc species reported in water hampers a deeper analysis of general trends.

With the current computational means, the calculations described in this paper can be easily performed to large data set of compounds, enabling for an accurate estimation of their acid-base properties. Moreover, discerning their different energy contributions to the pK_a values would prove essential to understand their intrinsic acidity and tune it by modulating their ligand environment.

Declaration of Competing Interest

The authors declare that they have no known competing financial interests or personal relationships that could have appeared to influence the work reported in this paper.

Acknowledgements

A. L. acknowledges financial support from Spanish Ministry of Science and Innovation (project PID-2020-116861GB-I00). M.A.O. acknowledges Xunta de Galicia (Investigador Distinguido program ED431H 2020/21, Centro singular de investigación de Galicia accreditation 2019-2022, ED431G 2019/03) and the European Union (European Regional Development Fund - ERDF).

Supplementary materials

Supplementary material associated with this article can be found, in the online version, at doi:10.1016/j.jorganchem.2021.121957.

References

[1] R. Coontz, B. Hanson, Not so simple, Science 305 (2004) 957, doi:10.1126/science.305.5686.957.

[2] G.J. Kubas, Five-co-ordinate molybdenum and tungsten complexes, $[M(CO)_3(PCy_3)_2]$, which reversibly add dinitrogen, dihydrogen, and other small molecules, J. Chem. Soc., Chem. Commun. (1980) 61–62, doi:10.1039/C39800000061.

[3] G.J. Kubas, R.R. Ryan, B.I. Swanson, P.J. Vergamini, H.J. Wasserman, Characterization of the first examples of isolable molecular hydrogen complexes, $M(CO)_3(PR_3)_2(H2)$ (M = molybdenum or tungsten; R = Cy or isopropyl). Evidence for a side-on bonded dihydrogen ligand, J. Am. Chem. Soc. 106 (1984) 451–452, doi:10.1021/ja00314a049.

[4] G.J. Kubas, Metal-Dihydrogen and σ-Bond Complexes: Structure, Bonding, and Reactivity, Kluwer Academic/Plenum, New York, 2001.

[5] G.J. Kubas, Dihydrogen complexes as prototypes for the coordination chemistry of saturated molecules, Proc. Natl. Acad. Sci. USA 104 (2007) 6901–6907, doi:10.1073/pnas.0609707104.

[6] G.J. Kubas, Fundamentals of H_2 binding and reactivity on transition metals underlying hydrogenase function and H_2 production and storage, Chem. Rev. 107 (2007) 4152–4205, doi:10.1021/cr050197j.

[7] G.J Kubas, Hydrogen activation on organometallic complexes and H_2 production, utilization, and storage for future energy, J. Organomet. Chem. 694 (2009) 2648–2653, doi:10.1016/j.jorganchem.2009.05.027.

[8] G.J. Kubas, The art and beauty of inorganic synthesis on the path to discovery: transition metal coordination and activation of sulfur dioxide and dihydrogen, Comm. Inorg. Chem. 33 (2012) 102–121, doi:10.1080/02603594.2013.772896.

[9] G.J. Kubas, Activation of dihydrogen and coordination of molecular H_2 on transition metals, J. Organomet. Chem. 751 (2013) 33–49, doi:10.1016/j.jorganchem.2013.07.041.

[10] G.J. Kubas, Metal-dihydrogen and sigma-bond coordination: the consummate extension of the Dewar-Chatt-Duncanson model for metal-olefin bonding, J. Organomet. Chem. 635 (2001) 37–68, doi:10.1016/S0022-328X(01)01066-X.

[11] D.M. Heinekey, A. Lledós, J.M. Lluch, Elongated dihydrogen complexes: what remains of the H-H Bond? Chem. Soc. Rev. 33 (2004) 175–182, doi:10.1039/b304879a.

[12] D. Devarajan, D.H. Ess, Metal-mediated dihydrogen activation. What determines the transition-state geometry? Inorg. Chem. 51 (2012) 6367–6375, doi:10.1021/ic3006426.

[13] R. Mas-Ballesté, A. Lledós, H–H bond activation, in: J. Reedijk, K. Poeppelmeier (Eds.), Comprehensive Inorganic Chemistry II, Vol 9. Oxford: Elsevier; 2013. pp. 727-766.

[14] N.V. Belkova, E.S. Shubina, L.M. Epstein, Diverse world of unconventional hydrogen bonds, Acc. Chem. Res. 38 (2005) 624–631, doi:10.1021/ar040006j.

[15] M. Besora, A. Lledós, F. Maseras, Protonation of transition-metal hydrides: a not so simple process, Chem. Soc. Rev. 38 (2009) 957–966, doi:10.1039/b608404b.

[16] O.A. Filippov, N.V. Belkova, L.M. Epstein, A. Lledos, E.S. Shubina, Directionality of dihydrogen bonds: the role of transition metal atoms, ChemPhysChem 13 (2012) 2677–2687, doi:10.1002/cphc.201200097.

[17] P.E.M. Siegbahn, J.W. Tye, M.B. Hall, Computational studies of [NiFe] and [FeFe] hydrogenases, Chem. Rev. 107 (2007) 4414–4435, doi:10.1021/cr050185y.

[18] J.C. Gordon, G.J. Kubas, Perspectives on how Nature employs the principles of organometallic chemistry in dihydrogen activation in hydrogenases, Organometallics 29 (2010) 4682–4701, doi:10.1021/om100436c.

[19] T. Liu, X. Wang, C. Hoffmann, D.L. DuBois, R.M. Bullock, Heterolytic cleavage of hydrogen by an iron hydrogenase model: an Fe-H···H-N dihydrogen bond characterized by neutron diffraction, Angew. Chem. Int. Ed. 53 (2014) 5300–5304, doi:10.1002/anie.201402090.

[20] E. Buncel, B. Menon, Carbanion mechanisms. 6. Metalation of arylmethanes by potassium hydride/18-crown-6 ether in tetrahydrofuran and the acidity of hydrogen, J. Am. Chem. Soc. 99 (1977) 4457–4461, doi:10.1021/ja00455a040.

[21] R.H. Morris, Brønsted–Lowry, Acid strength of metal hydride and dihydrogen, complexes, Chem. Rev. 116 (2016) 8588–8654, doi:10.1021/acs.chemrev.5b00695.

[22] M.S. Chinn, D.M. Heinekey, Synthesis and properties of a series of ruthenium dihydrogen complexes, J. Am. Chem. Soc. 109 (1987) 5865–5867, doi:10.1021/ja00253a057.

[23] G. Jia, R.H. Morris, Wide range of pKa values of coordinated dihydrogen. Synthesis and properties of some η^2-dihydrogen and dihydride complexes of ruthenium, J. Am. Chem. Soc. 113 (1991) 875–883, doi:10.1021/ja00003a022.

[24] E.P. Cappellani, S.D. Drouin, G. Jia, P.A. Maltby, R.H. Morris, C.T. Schweitzer, Effect of the ligand and metal on the pKa values of the dihydrogen ligand in the series of Complexes $[M(H_2)H(L)_2]^+$, M = Fe, Ru, Os, containing isosteric ditertiaryphosphine ligands, L, J. Am. Chem. Soc. 116 (1994) 3375–3388, doi:10.1021/ja00087a024.

[25] P.A. Maltby, M. Schlaf, M. Steinbeck, A.J. Lough, R.H. Morris, W.T. Klooster, T.F. Koetzle, R.C. Srivastava, Dihydrogen with frequency of motion near the ^{1}H Larmor frequency. Solid-state structures and solution NMR spectroscopy of osmium complexes trans-$[Os(H{\bullet\bullet}H)X(PPh_2CH_2CH_2PPh_2)_2]^+$ (X = Cl, Br), J. Am. Chem. Soc. 118 (1996) 5396–5407, doi:10.1021/ja9529044.

[26] D.G. Gusev, R. Hübener, P. Burger, O. Orama, H. Berke, Synthesis, structural diversity, dynamics, and acidity of the M(II) and M(IV) Complexes $[MH_3(PR_3)_4]^+$ (M = Fe, Ru, Os; R = Me, Et), J. Am. Chem. Soc. 119 (1997) 3716–3731, doi:10.1021/ja963692t.

[27] G. Jia, H.M. Lee, I.D. Williams, C.P. Lau, Y. Chen, Synthesis, characterization, and acidity properties of $[MCl(H_2)(L)(PMP)]BF_4$ (M = Ru, L = PPh_3, CO; M = Os, L = PPh_3; PMP = 2,6-$(Ph_2PCH_2)_2C_5H_3N$), Organometallics 16 (1997) 3941–3949, doi:10.1021/om970207+.

[28] S.M. Ng, Y.Q. Fang, C.P. Lau, W.T. Wong, G. Jia, Synthesis, characterization, and acidity of ruthenium dihydrogen complexes with 1,4,7-triazacyclononane, 1,4,7-trimethyl-1,4,7-triazacyclononane, and hydrotris(pyrazolyl)borato ligands, Organometallics 17 (1998) 2052–2059, doi:10.1021/om9710374.

[29] W.S. Ng, G. Jia, M.Y. Hung, C.P. Lau, K.Y. Wong, L. Wen, Ligand effect on the structures and scidities of $[TpOs(H_2)(PPh_3)_2]BF_4$ and $[CpOsH_2(PR_3)_2]BF_4$„ Organometallics 17 (1998) 4556–4561, doi:10.1021/om9804071.

[30] G. Jia, C.P. Lau, P C., Structural, acidity and chemical properties of some dihydrogen/hydride complexes of Group 8 metals with cyclopentadienyls and related ligands, Coord. Chem. Rev. 190-192 (1999) 83–108, doi:10.1016/S0010-8545(99)00066-1.

[31] K. Abdur-Rashid, T.P. Fong, B. Greaves, D.G. Gusev, J.G. Hinman, S.E. Landau, A.J. Lough, R.H. Morris, An acidity scale for phosphorus-containing compounds including metal hydrides and dihydrogen complexes in THF: toward the unification of acidity scales, J. Am. Chem. Soc. 122 (2000) 9155–9171, doi:10.1021/ja994428d.

[32] K.K. Majumdar, H.V. Nanishankar, B.R. Jagirdar, Some new dicationic dihydrogen complexes of ruthenium, Eur. J. Inorg. Chem. (2001) 1847–1853, doi:10.1002/1099-0682(200107)2001:7≤1847::AID-EJIC1847≥3.0.CO;2-Q.

[33] T. Li, A.J. Lough, C. Zuccaccia, A. Macchioni, R.H. Morris, An acidity scale of phosphonium tetraphenylborate salts and ruthenium dihydrogen complexes in dichloromethane, Can. J. Chem. 84 (2006) 164–175, doi:10.1139/v05-236.

[34] M.S. Chinn, D.M. Heinekey, N.G. Payne, C.D. Sofield, Highly reactive dihydrogen complexes of ruthenium and rhenium: facile heterolysis of coordinated dihydrogen, Organometallics 8 (1989) 1824–1826, doi:10.1021/om00109a042.

[35] E.R. Rocchini, A. Mezzetti, H. Rüegger, U. Burckhardt, V. Gramlich, A. del Zotto, P. Martinuzzi, P. Rigo, Heterolytic H_2 activation by dihydrogen complexes. Effects of the ligand X in $[M(X)H_2\{Ph_2P(CH_2)_3PPh_2\}_2]^{n+}$ (M = Ru, Os; X = CO, Cl, H), Inorg. Chem. 36 (1997) 711–720, doi:10.1021/ic9605579.

[36] M. Schlaf, A.J. Lough, P.A. Maltby, R.H. Morris, Synthesis, structure, and properties of the stable and highly acidic dihydrogen complex trans-$[Os(\eta^2-H_2)(CH_3CN)(dppe)_2](BF_4)_2$. Perspectives on the influence of the trans ligand on the chemistry of the dihydrogen ligand, Organometallics 15 (1996) 2270–2278, doi:10.1021/om960113k.

[37] R.H. Morris, Estimating the acidity of transition metal hydride and dihydrogen complexes by adding ligand acidity constants, J. Am. Chem. Soc. 136 (2014) 1948–1959, doi:10.1021/ja410718r.

[38] M.M.H. Sung, R.H. Morris, Density Functional Theory calculations support the additive nature of ligand contributions to the pK_a of iron hydride phosphine carbonyl complexes, Inorg. Chem. 55 (2016) 9596–9601, doi:10.1021/acs.inorgchem.6b01274.

[39] J.P. Unsleber, J. Neugebauer, R.H. Morris, DFT methods applied to answer the question: how accurate is the ligand acidity constant method for estimating the pKa of transition metal hydride complexes MHXL4 when X is varied? Dalton Trans. 47 (2018) 2739–2747, doi:10.1039/c7dt03473c.

[40] M.M.H. Sung, S. Jdanova, R.H. Morris, Ligand acidity constants as calculated by density functional theory for PF_3 and N-Heterocyclic carbene ligands in hydride complexes of iron(II), J. Organomet. Chem. 880 (2019) 15–21, doi:10.1016/j.jorganchem.2018.10.024.

[41] N.K. Szymczak, D.R. Tyler, Aspects of dihydrogen coordination chemistry relevant to reactivity in aqueous solution, Coord. Chem. Rev. 252 (2008) 212–230, doi:10.1016/j.ccr.2007.06.007.

[42] K.S. Alongi, G.C. Shields, Theoretical calculations of acid dissociation constants: a review article, Ann. Rep. Comp. Chem. 6 (2010) 113–138, doi:10.1016/S1574-1400(10)06008-1.

[43] J. Ho, M.L. Coote, A universal approach for continuum solvent pK a calculations: are we there yet? Theor. Chem. Acc. 125 (2010) 3–21, doi:10.1007/s00214-009-0667-0.

[44] J. Ho, M.L. Coote, First-principles prediction of acidities in the gas and solution phase, WIREs Comput. Mol. Sci. 1 (2011) 649–660, doi:10.1002/wcms.43.

[45] P.G. Seybold, G.C. Shields, Computational estimation of pKa values, WIREs Comput. Mol. Sci. 5 (2015) 290–297 5https://doi.org/, doi:10.1002/wcms.1218.

[46] V. Sinha, J.J. Laan, E.A. Pidko, Accurate and rapid prediction of pK_a of transition metal complexes: semiempirical quantum chemistry with a data-augmented approach, Phys. Chem. Chem. Phys. 23 (2021) 2557–2567, doi:10.1039/d0cp05281g.

[47] F. Creati, C. Coletti, N. Re, Density Functional study of butadiyne to butatrienylidene isomerization in $[Ru(HC{\equiv}CC{\equiv}CH)(PMe_3)_2(Cp)]^+$, Organometallics 28 (2009) 6603–6616, doi:10.1021/om9007295.

[48] M. Jiménez-Tenorio, M.C. Puerta, P. Valerga, M.A. Ortuño, G. Ujaque, A. Lledós, Counteranion and solvent assistance in ruthenium-mediated alkyne to vinylidene isomerizations, Inorg. Chem. 52 (2013) 8919–8932, doi:10.1021/ic401119p.

[49] G. Kovács, A. Rossin, L. Gonsalvi, A. Lledós, M. Peruzzini, Comparative DFT analysis of ligand and solvent effects on the mechanism of H_2 activation in water mediated by half-sandwich Complexes $[Cp'Ru(PTA)_2Cl]$ (Cp' = C_5H_5, C_5Me_5; PTA=1,3,5-triaza-7-phosphaadamantane), Organometallics 29 (2010) 5121–5131, doi:10.1021/om100326z.

[50] J. Díez, J. Gimeno, A. Lledós, F.J. Suárez, C. Vicent, Imidazole based ruthenium(IV) complexes as highly efficient bifunctional catalysts for the redox isomerization of allylic alcohols in aqueous medium: water as cooperating ligand, ACS Catal. 2 (2012) 2087–2099, doi:10.1021/cs300369j.

[51] A.S. Guan, I.X. Liang, C.X. Zhou, T.R. Cundari, Metal and ligand effects on coordinated methane pK_a: direct correlation with the methane activation barrier, J. Phys. Chem. A 124 (2020) 7283–7289, doi:10.1021/acs.jpca.0c04756.

[52] J.D. Gilbertson, N.K. Szymczak, D.R. Tyler, H_2 activation in aqueous solution: formation of trans-$[Fe(DMeOPrPE)_2H(H_2)]^+$ via the heterolysis of H_2 in water, Inorg. Chem. 43 (2004) 3341–3343, doi:10.1021/ic0498642.

[53] J.D. Gilbertson, N.K. Szymczak, J.L. Crossland, W.K. Miller, D.K. Lyon, B.M. Foxman, J. Davis, D.R. Tyler, Coordination chemistry of H_2 and N_2 in aqueous solution. Reactivity and mechanistic studies using trans-$Fe^{II}(P_2)_2X_2$-type complexes (P_2 = a chelating, water-solubilizing phosphine), Inorg. Chem. 46 (2007) 1205–1214, doi:10.1021/ic061570o.

[54] D.N. Akbayeva, L. Gonsalvi, W. Oberhauser, M. Peruzzini, F. Vizza, P. Brüggeller, A. Romerosa, G. Sava, A. Bergamo, Synthesis, catalytic properties and biological activity of new water soluble ruthenium cyclopentadienyl PTA complexes $[(C_5R_5)RuCl(PTA)_2]$ (R = H, Me; PTA = 1,3,5-triaza-7-phosphaadamantane), Chem. Commun. (2003) 264–265, doi:10.1039/B210102E.

[55] A. Rossin, L. Gonsalvi, A.D. Phillips, O. Maresca, A. Lledós, M. Peruzzini, Water-assisted H-H bond splitting mediated by $[CpRu(PTA)_2Cl]$ (PTA=1,3,5-triaza-7-phosphaadamantane). A DFT analysis, Organometallics 26 (2007) 3289–3296, doi:10.1021/om061023a.

[56] N.K. Szymczak, L.N. Zakharov, D.R. Tyler, Solution chemistry of a water-soluble η^2-H_2 ruthenium complex: evidence for coordinated H_2 acting as a hydrogen bond donor, J. Am. Chem. Soc. 128 (2006) 15830–15835, doi:10.1021/ja065532f.

[57] N.K. Szymczak, D.A. Braden, J.L. Crossland, Y. Turov, L.N. Zakharov, D.R. Tyler, Aqueous coordination chemistry of H_2: why is coordinated H_2 inert to substitution by water in trans-$Ru(P_2)_2(H_2)H^+$-type Complexes (P_2 = a chelating phosphine)? Inorg. Chem. 48 (2009) 2976–2984, doi:10.1021/ic801884x.

[58] C.M. Nagaraja, M. Nethaji, B.R. Jagirdar, Highly Electrophilic, 16-electron $[Ru(P(OMe)(OH)_2)(dppe)_2]^{2+}$ complex turns $H_2(g)$ into a strong acid and splits a Si–H bond heterolytically. Synthesis and structure of the novel phosphorous acid complex $[Ru(P(OH)_3)(dppe)_2]^{2+}$, Inorg. Chem. 44 (2005) 4145–4147, doi:10.1021/ic050026x.

[59] N. Aebischer, U. Frey, A.E. Merbach, Formation and in situ characterization of the first dihydrogen aqua complex: $[Ru(H_2O)_5(H_2)]^{2+}$, Chem. Commun. (1998) 2303–2304, doi:10.1039/A805579C.

[60] J. Malin, H. Taube, Ion dihydridobis(ethylenediamine)osmium(IV), Inorg. Chem. 10 (1971) 2403–2406, doi:10.1021/ic50105a007.

[61] W.D. Harman, H. Taube, Isostructural η^2-dihydrogen complexes $[Os(NH_3)_5(H_2)]^{n+}$ (n = 2, 3) and the hydrogenation of acetone, J. Am. Chem. Soc. 112 (1990) 2261–2263, doi:10.1021/ja00162a028.

[62] Z.-W. Li, H. Taube, Modulation of physical and chemical properties of η^2-H_2 complexes of osmium ammines by facile substitution, J. Am. Chem. Soc. 113 (1991) 8946–8947, doi:10.1021/ja00023a052.

[63] Y. Zhao, D.G. Truhlar, The M06 suite of density functionals for main group thermochemistry, thermochemical kinetics, noncovalent interactions, excited states, and transition elements: two new functionals and systematic testing of four M06-class functionals and 12 other functionals, Theor. Chem. Acc. 120 (2008) 215–241, doi:10.1007/s00214-007-0310-x.

[64] S.E. Wheeler, K.N. Houk, Integration grid errors for meta-GGA-predicted reaction energies: origin of grid errors for the M06 suite of functionals, J. Chem. Theory Comput. 6 (2010) 395–404, doi:10.1021/ct900639j.

[65] M.J. Frisch, G.W. Trucks, H.B. Schlegel, G.E. Scuseria, M.A. Robb, J.R. Cheeseman, G. Scalmani, V. Barone, G.A. Petersson, H. Nakatsuji, X. Li, M. Caricato, A. Marenich, J. Bloino, B.G. Janesko, R. Gomperts, B. Mennucci, H.P. Hratchian, J.V. Ortiz, A.F. Izmaylov, J.L. Sonnenberg, D. Williams-Young, F. Ding, F. Lipparini, F. Egidi, J. Goings, B. Peng, A. Petrone, T. Henderson, D. Ranasinghe, V.G. Zakrzewski, J. Gao, N. Rega, G. Zheng, W. Liang, M. Hada, M. Ehara, K. Toyota, R. Fukuda, J. Hasegawa, M. Ishida, T. Nakajima, Y. Honda, O. Kitao, H. Nakai, T. Vreven, K. Throssell, J.A. Montgomery Jr., J.E. Peralta, F. Ogliaro, M. Bearpark, J.J. Heyd, E. Brothers, K.N. Kudin, V.N. Staroverov, T. Keith, R. Kobayashi, J. Normand, K. Raghavachari, A. Rendell, J.C. Burant, S.S. Iyengar, J. Tomasi, M. Cossi, J.M. Millam, M. Klene, C. Adamo, R. Cammi, J.W. Ochterski, R.L. Martin, K. Morokuma, O. Farkas, J.B. Foresman, D.J. Fox, Gaussian 09, Revision A.02, Gaussian, Inc., Wallingford CT, 2016.

[66] Y. Zhao, Y.D.G. Truhlar, Density functionals with broad applicability in chemistry, Acc. Chem. Res. 41 (2008) 157–167, doi:10.1021/ar700111a.

[67] Y. Zhao, D.G. Truhlar, Applications and validations of the Minnesota density functionals, Chem. Phys. Lett. 502 (2011) 1–13, doi:10.1016/j.cplett.2010.11.060.

[68] V.S. Bryantsev, M.S. Diallo, A.C.T. van Duin, W.A. Goddard III, Evaluation of B3LYP, X3LYP, and M06-class density functionals for predicting the binding energies of neutral, protonated, and deprotonated water clusters, J. Chem. Theory Comput. 5 (2009) 1016–1026, doi:10.1021/ct800549f.

[69] D. Andrae, U. Häußermann, M. Dolg, H. Stoll, H. Preuß, Energy-adjusted ab initio pseudopotentials for the second and third row transition elements, Theor. Chim. Acta 77 (1990) 23–141, doi:10.1007/BF01114537.

[70] A.W. Ehlers, M. Böhme, S. Dapprich, A. Gobbi, A. Höllwarth, V. Jonas, K.F. Köhler, R. Stegmann, A. Veldkamp, G. Frenking, A set of f-polarization functions for pseudo-potential basis sets of the transition metals Sc-Cu, Y-Ag and La-Au, Chem. Phys. Lett. 208 (1993) 111–114, doi:10.1016/0009-2614(93)80086-5.

[71] W.J. Hehre, R. Ditchfield, J.A. Pople, Self–consistent molecular orbitalm. XII. Further extensions of gaussian–type basis sets for use in molecular orbital studies of organic molecules, J. Chem. Phys. 56 (1972) 2257–2261, doi:10.1063/1.1677527.

[72] P.C. Hariharan, J.A. Pople, The influence of polarization functions on molecular orbital hydrogenation energies, Theor. Chim. Acta 28 (1973) 213–222, doi:10.1007/BF00533485.

[73] M.M. Francl, W.J. Pietro, W.J. Hehre, J.S. Binkley, M.S. Gordon, D.J. DeFrees, J.A. Pople, Self-consistent molecular orbital methods. XXIII. A polarization-type basis set for second-row elements, J. Chem. Phys. 77 (1982) 3654–3665, doi:10.1063/1.444267.

[74] R. Krishnan, J.S. Binkley, R. Seeger, J.A. Pople, Self-consistent molecular orbital methods. XX. A basis set for correlated wave functions, J. Chem. Phys. 72 (1980) 650–654, doi:10.1063/1.438955.

[75] A.D. McLean, G.S. Chandler, Contracted Gaussian basis sets for molecular calculations. I. Second row atoms, Z=11–18, J. Chem. Phys. 72 (1980) 5639–5648, doi:10.1063/1.438980.

[76] T. Clark, J. Chandrasekhar, G.W. Spitznagel, P.v.R. Schleyer, Efficient diffuse function-augmented basis sets for anion calculations. III. The 3-21+G basis set for first-row elements, Li–F, J. Comp. Chem. 4 (1983) 294–301, doi:10.1002/jcc.540040303.

[77] A.V. Marenich, C.J. Cramer, D.G. Truhlar, Universal solvation model based on solute electron density and on a continuum model of the solvent defined by the bulk dielectric constant and atomic surface tensions, J. Phys. Chem. B 113 (2009) 6378–6396, doi:10.1021/jp810292n.

[78] J.R. Pliego, J.M. Riveros, Theoretical calculation of pKa using the cluster–continuum model, J. Phys. Chem. A 106 (2002) 434–7439, doi:10.1021/jp025928n.

[79] C.P. Kelly, C.J. Cramer, D.G. Truhlar, Adding explicit solvent molecules to continuum solvent calculations for the calculation of aqueous acid sissociation constants, J. Phys. Chem. A 110 (2006) 2493–2499, doi:10.1021/jp055336f.

[80] J.R. Pliego, J.M. Riveros, The cluster–continuum model for the calculation of the solvation free energy of ionic species, J. Phys. Chem. A 105 (2001) 7241–7247, doi:10.1021/jp004192w.

[81] C.-G. Zhan, D.A. Dixon, Absolute hydration free energy of the proton from first-principles electronic structure calculations, J. Phys. Chem. A 105 (2001) 11534–11540, doi:10.1021/jp012536s.

[82] V.S. Bryantsev, M.S. Diallo, W.A. Goddard III, Calculation of solvation free energies of charged solutes using mixed cluster/continuum models, J. Phys. Chem. B 112 (2008) 9709–9719, doi:10.1021/jp802665d.

[83] C.P. Kelly, C.J. Cramer, D.G. Truhlar, Aqueous solvation free energies of ions and ion–water clusters based on an accurate value for the absolute aqueous solvation free energy of the proton, J. Phys. Chem. B 110 (2006) 16066–16081, doi:10.1021/jp063552y.

[84] J.R. Pliego Jr., J.M. Riveros, Hybrid discrete-continuum solvation methods, WIREs Comput. Mol. Sci. 10 (2020) e1440, doi:10.1002/wcms.1440.

[85] 1.9 kcal mol^{-1} at 298.15 K: C.P. Kelly, C.J. Cramer, D.G. Truhlar, SM6: A Density Functional Theory continuum solvation model for calculating aqueous solvation free energies of neutrals, ions, and solute–water clusters, J. Chem. Theory Comput. 1 (2005) 1133–1152, doi:10.1021/ct050164b.

[86] [water] = 55.34 M; [THF] 12.3 M

[87] M.D. Tissandier, K.A. Cowen, W.Y. Feng, E. Gundlach, M.H. Cohen, A.D. Earhart, J.V. Coe, T.R. Tuttle Jr., The proton's absolute aqueous enthalpy and Gibbs free energy of solvation from cluster-ion solvation data, J. Phys. Chem. A 102 (1998) 7787–7794, doi:10.1021/jp982638r.

[88] D.M. Camaioni, C.A. Schwerdtfeger, Comment on "Accurate experimental values for the free energies of hydration of H^+, OH^-, and $H3O^+$", J. Phys. Chem. A 109 (2005) 10795–10797, doi:10.1021/jp054088k.

[89] Some authors claim for more negative values in aqueous and non-aqueous solvents R. Bhattacharyya, S.C. Lahiri, Comparative study of the absolute values of enthalpy and Gibbs free energy of solvation of proton from cluster-ion solvation data and direct determination of the thermodynamic parameters of proton in aqueous and non-aqueous solvents, Z. Phys. Chem. 224 (2010) 1389–1410, doi:10.1524/zpch.2010.5547.

[90] Y. Markus, Thermodynamic functions of transfer of single ions from water to nonaqueous solvents: part 1 – Gibbs free energies of transfer to nonaqueous solvents, Pure Appl. Chem. 55 (1983) 977–1021, doi:10.1351/pac198355060977.

[91] B. Bandow, B. Hartke, Larger water clusters with edges and corners on their way to ice: structural trends elucidated with an improved parallel evolutionary algorithm, J. Phys. Chem. A 110 (2006) 5809–5822, doi:10.1021/jp060512l.

[92] U. Buck, C.C. Pradzynski, T. Zeuch, J.M. Dieterichc, B. Hartke, A size resolved investigation of large water clusters, Phys. Chem. Chem. Phys. 16 (2014) 6859–6871, doi:10.1039/C3CP55185G.

[93] E.E. Dahlke, R.M. Olson, H.R. Leverentz, D.G. Truhlar, Assessment of the accuracy of Density Functionals for prediction of relative energies and geometries of low-lying isomers of water hexamers, J. Phys. Chem. A 112 (2008) 3976–3984, doi:10.1021/jp077376k.

[94] J.T. Su, X. Xu, W.A. Goddard III, Accurate energies and structures for large water clusters using the X3LYP hybrid Density Functional, J. Phys. Chem. A 108 (2004) 10518–10526, doi:10.1021/jp047502+.

[95] A.L. Sobolewski, W. Domcke, Ab Initio investigation of the structure and spectroscopy of hydronium–water clusters, J. Phys. Chem. A 106 (2002) 4158–4167, doi:10.1021/jp013835k.

[96] E.S. Stoyanov, I.V. Stoyanova, C.A. Reed, The Structure of the hydrogen ion (H_{aq}^+) in water, J. Am. Chem. Soc. 132 (2010) 1484–1485, doi:10.1021/ja9101826.

[97] E.S. Stoyanov, I.V. Stoyanova, C.A. Reed, The unique nature of H^+ in water, Chem. Sci. 2 (2011) 462–472, doi:10.1039/C0SC00415D.

[98] C.A. Reed, Myths about the proton. The nature of H^+ in condensed media, Acc. Chem. Res. 46 (2013) 2567–2575, doi:10.1021/ar400064q.

[99] Geometry optimization in the gas phase. Experimental studies report slightly larger O–O distances, ca. 2.5–2.6 Å [96-98].

[100] Previous calculations [49]for species **3** and **4** —using B3LYP/PCM level of theory and a cluster of 4 water molecules— provided somehow lower pKawater values, but the difference of 1.6 units between Cp and Cp* derivatives agree with the current result of 1.3.
[101] J.R. Sowa, R.J. Angelici, Bidentate phosphine basicities as determined by enthalpies of protonation, Inorg. Chem. 30 (1991) 3534–3537, doi:10.1021/ic00018a027.
[102] J.R. Sowa, V. Zanotti, G. Facchin, R.J. Angelici, Calorimetric studies of the heats of protonation of the metal in $Fe(CO)_3$(bidentate phosphine, arsine) complexes: effects of chelate ligands on metal basicity, J. Am. Chem. Soc. 114 (1992) 160–165, doi:10.1021/ja00027a023.